UDC 539.23; 539.216.1

E.S.Platonova[1], V.Buchinskas[2], V.M.Jurov[3], V.Ch.Laurinas[3]

[1]*Karaganda State Technical University;*
[2]*Vilnius Gediminas Technical University, Lithuania;*
[3]*Ye.A.Buketov Karaganda State University*
(E-mail: exciton@list.ru)

Technology deposition of corrosion-resistant and scratch-resistant coating on the details of mining equipment

As it is shown experimentally that the technology greatly exceeds the vacuum nitriding zinc coatings. Along with this, the cost of such parts with coatings 10–15 % lower zinc. From the experimental data that the Fe–Al coating and Fe–Al–Ti can be used as corrosion-resistant, anti-friction coatings on low-grade steels. This increases the life of the components of these steels in 3–4 times. Compare the result of nanohardness (7.413 GPa) with known solid materials shows that nanohardness coating Cr–Mn–Si–Cu–Fe–Al is almost 2 times higher nanohardness titanium and close to the multi-layer film Ti/α-C:H. Comparing the measurement results with the microhardness of the coating Fe–Al, Fe–Al–Ti and other shows that the multilayer coating is significantly superior to the latter. After nitriding microhardness multilayer coating increases.

Key words: coating, nitriding, microhardness, nanohardness, corrosion resistance, heat resistance, friction.

Introduction

Currently, with limited material resources in the industrial complex are particularly important technologies that increase the durability (life) of parts and units of machines. 90 % of parts and machines out of order due to surface wear. This is especially true for the mining and oil field equipment, equipment and energy complex, where the majority of mechanisms operate in extreme conditions, and in particular, in a high abrasion and high temperatures.

The most relevant and promising to produce nanostructured hardening, wear-resistant, corrosion-resistant and heat-resistant coatings are vacuum ion-plasma methods: magnetron sputtering, ion and vacuum arc deposition [1–17]. This is due to the fact that in addition there are thermal factors and other — the high degree of ionization, the flux density and particle energy. The quality of the coating can be adjusted by changing the substrate temperature, pressure of the working gas, the potential of the substrate and other process parameters.

This paper presents experimental results on the application of anticorrosive and strengthening coatings on parts of mining equipment.

Titanium nitride coating

In parts of mining equipment (steel 35) were coated TiN. Figure 1 shows a typical structure of a titanium nitride coating obtained with an optical microscope, which clearly shows the microcrystals TiN. There is a small amount and droplet phase.

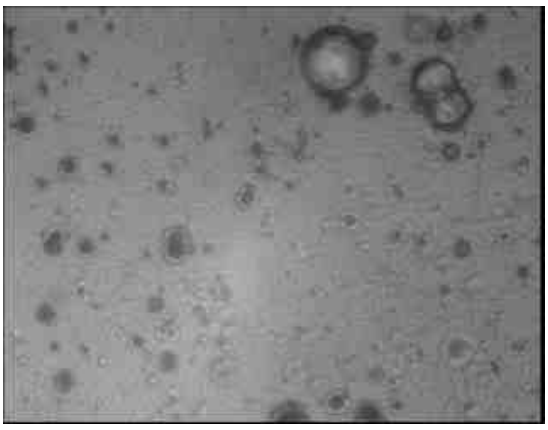

Figure 1. Snapshot TiN coating for details (increasing ×400)

Table 1 shows corrosion rates for parts made of steel 35.

Table 1

The corrosion rate of titanium nitride coatings in industrial environments

Environment	Concentration, % (by weight)	Temperature, ºC	Corrosion rate mm/year
Nitric acid	80	20	0,01
Sulfuric acid	52	20	0,03
Hydrochloric acid	80	20	0,05

However, the calculation of economic efficiency of the entire production cycle of the application of titanium nitride coatings showed that the price of the above items of mining equipment, increased by approximately 20 % compared to galvanized coatings.

One of the methods of chemical and heat treatment of steel parts is the method of ion-plasma nitriding. Table 2 shows the comparative analysis.

Table 2

Characteristics of various coatings

Name details	Anti-corrosion coating	K-Factor
Coupling RU11.008–01, Steel 35	Zinc	0,15
Coupling RU11.008–01, Steel 35	Nitrated	0,40
Coupling RU11.008–01, Steel 35	Titanium nitride	0,75

Table 2 shows that the vacuum nitriding technology, though inferior in the corrosion resistance of a titanium nitride coating, but much greater than zinc coating. Along with this, the cost of such parts with coatings (10 ÷ 15)% lower zinc.

Coatings Al–Fe and Al–Fe–Ti

Figures 2 and 3 show electron microscopic images coatings Al-Fe-Ti argon and nitrogen.

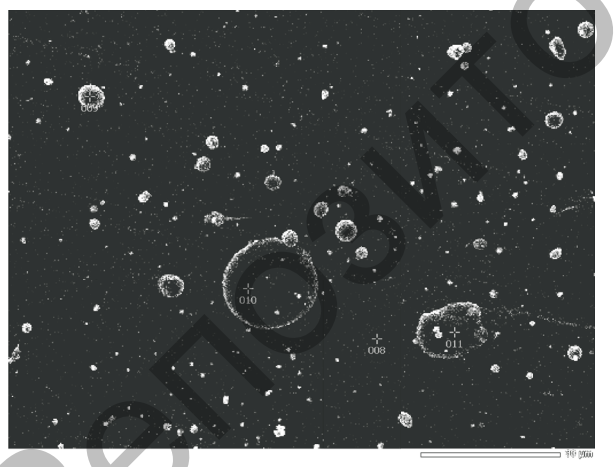

Figure 2. An electron microscope image of the coating Al–Fe–Ti in an argon atmosphere

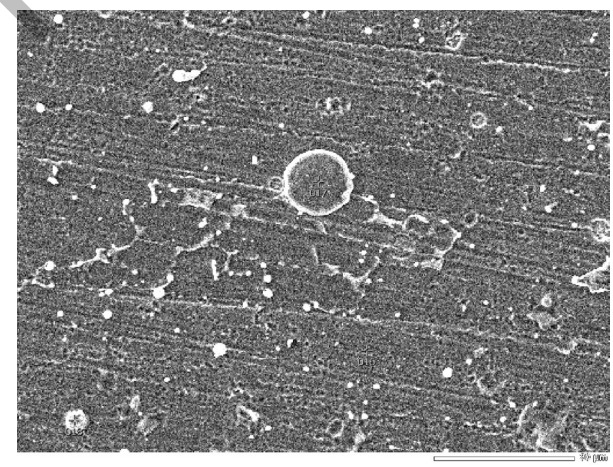

Figure 3. Electron microscope image of the coating Al–Fe–Ti in an argon atmosphere

In the first case, the average grain size of the titanium shell surrounded amorphous amounts 100–150 nm. Such coatings are called submicrocrystalline. The second case is the formation of mainly titanium nitride and iron. The grain size of about 50 nm. Such coatings are called nanocrystalline. Nitration covering Al–Fe leads to a change in its structure due to the formation of nitride phase (Fig. 4).

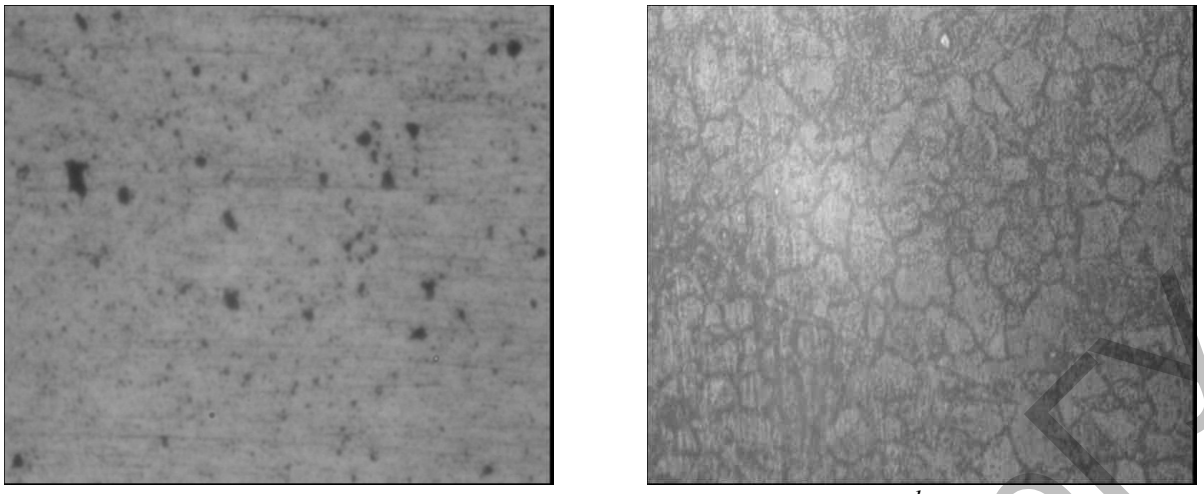

a *b*

Figure 4. Pictures Al–Fe coating before (*a*) and after (*b*) nitriding

The microhardness of the coating to Al–Fe nitriding is 245.6 MPa, and after the nitriding — 350.9 MPa, i.e. it increased by almost 1.5 times. Results of research on the heat resistance of coatings Al–Fe and Al–Fe–Ti are shown in Table 3. Heat resistance was evaluated by weight of the oxidized coating. Doping with Al–Fe coating titanium significantly affect its fire resistance. However synthesized significantly increase the heat resistance of the coating compared to an uncoated sample, approximately 4 times. Table 4 shows the characteristics of corrosion resistance studied in this paper covers some parts of mining equipment. Here, the coefficient K is determined by anodic polarization defects and initiate changes from $K = 0$ (for poor coating) to $K = 1$ (for quality coatings).

Table 3

The weight loss of the coating after heat treatment at 600 ºC for 100 hours

Coating	Weight oxidized coating, mg
Steel 35 uncoated	56,8
Fe–Al	14,2
Fe–Al–Ti (argon)	15,4
Fe–Al–Ti (nitrogen)	11,2

Table 4

Characteristics of various coatings

Name details	Anti-corrosion coating	K-Factor
Steel 35	Uncoating	0,14
Nipple 12, Steel 35	Fe-Al	0,47
Coupling 12 c, Steel 35	Fe-Al	0,54
Cork HLG 30.002 Steel 35	Fe-Al-Ti	0,69

Coating Zn–Al and Zn–Al–Ti

As an example, in Figure 5 shows the microstructure of the coating Zn–Al–Ti, prepared under a nitrogen atmosphere.

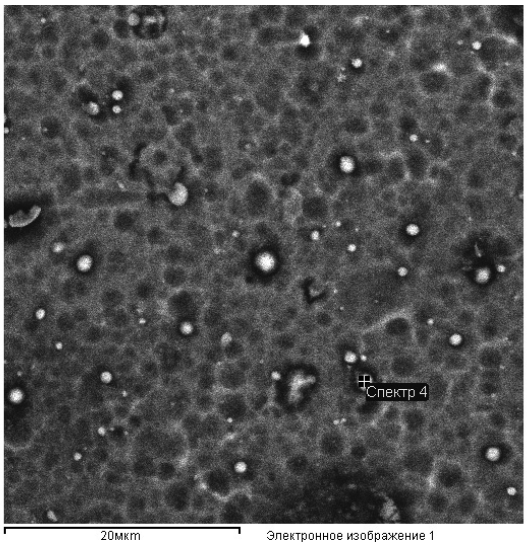

Figure 5. Electron microscope image of the coating Zn–Al–Ti, resulting in nitrogen and tested for heat resistance at 600 ºC for 100 hours

The titanium content in the coating according to XPS (Fig. 6) is 70 % iron and aluminum — about 14 % of oxygen and zinc just over 1 %. From Figure 5 clearly visible grains of titanium nitride, representing inclusions nano- and submicrocrystalline phase, surrounded by an amorphous layer.

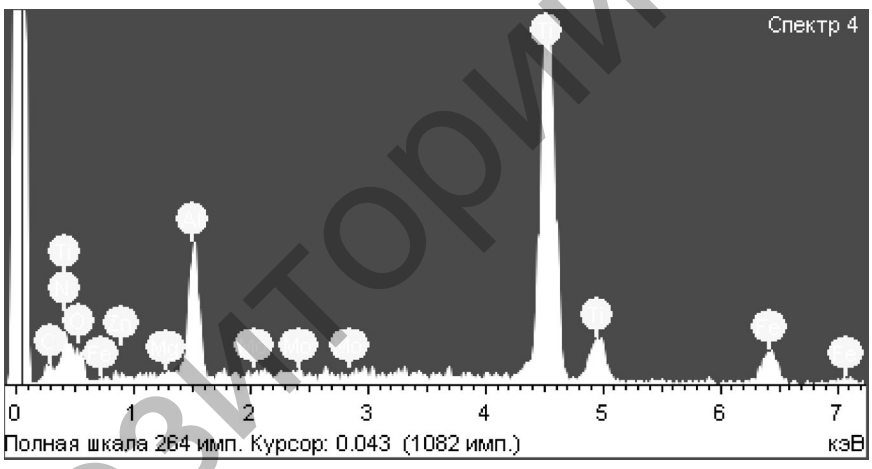

Figure 6. XPS coating Zn–Al–Ti, resulting in nitrogen and tested for heat resistance at 600 ºC for 100 hours

Loss of coating weight of Zn–Al–Ti, prepared under argon, and tested for heat resistance at 600 ºC for 100 hours is 0.6 mg and the coating produced in nitrogen — 0.3 mg.

Thus, the heat resistance of the coating Zn–Al–Ti, resulting in nitrogen and tested for heat resistance at 600 °C for 100 hours, almost 10 times the heat-resistant steel 12X18N10T.

Coatings Cr–Mn–Si–Cu–Fe–Al and Cr–Mn–Si–Cu–Fe–Al–Ti

Figure 7 shows an electron microscope image of the coating. To measure coating thickness Cr–Mn–Si–Cu–Fe–Al on its surface was cut by a focused ion beam marketplace. The layer thickness of 1 mm. Figure 8 shows the thickness of the coating Cr–Mn–Si–Cu–Fe–Al.

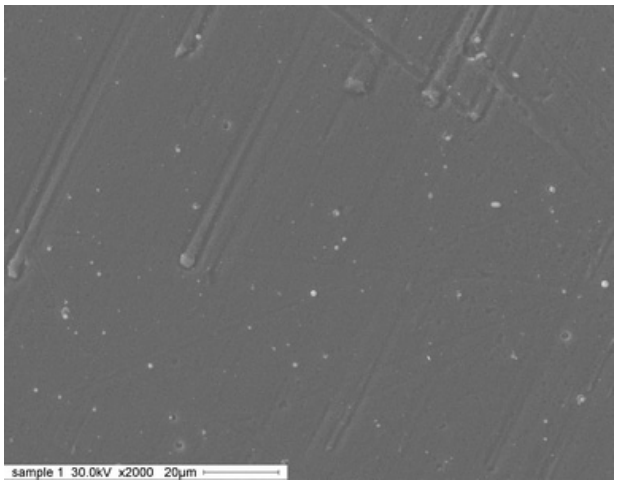

Figure 7. Electron microscope image of the coating Cr–Mn–Si–Cu–Fe–Al

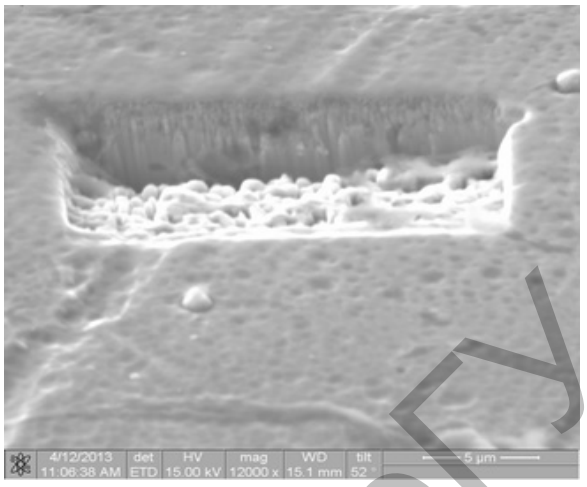

Figure 8. The thickness of the coating Cr–Mn–Si–Cu–Fe–Al

Results of the study of the phase composition and structural parameters of the sample are given in Table 5. The coating was determined nanohardness Cr–Mn–Si–Cu–Fe–Al in a gaseous environment of nitrogen, which is equal to 7.413 GPa, corresponding to 686.57 units according to the method of Vickers hardness. It has been determined: modulus strength of the coating which is equal to 169.51 GPa fluidity is 0.68 %, and the relaxation of the coating is 0.05 %. To determine all the above parameters were determined by Poisson's ratio for the coating Cr–Mn–Si–Cu–Fe–Al in a gas atmosphere of nitrogen of approximately 0.30.

Table 5

Phase composition of the coating Cr-Mn-Si-Cu-Fe-Al in a gaseous environment of nitrogen

Sample	Phase detection	The content of the phase, %	The lattice parameters, Å	$\Delta d/d \cdot 10^{-3}$
Cr–Mn–Si–Cu–Fe–Al in N_2 atmosphere	$FeN_{0.0324}$	60.6	a = 3.598	3.460
	$TiN_{0.31}O_{0.31}$	39.4	a = 4.211	5.143

It is interesting to compare the results with the known data on the nanoindentation other materials. These data are presented in Table 6.

Comparison of our results (7.413 GPa) with a table 6 shows that nanohardness coating Cr–Mn–Si–Cu–Fe–Al is almost 2 times higher nanohardness titanium and close to the multi-layer film Ti/α-C:H. However, the production of such a film is much harder than the coating Cr–Mn–Si–Cu–Fe–Al using composite cathode which without difficulty can be obtained by induction melting.

Also investigated were the coatings obtained cathode sputtering Cr–Mn–Si–Cu–Fe–Al in an argon atmosphere, and the coatings obtained by spraying while the cathode Cr–Mn–Si–Cu–Fe–Al and a titanium cathode mark.

Table 6

Properties of materials designed according nanoindentation

Material	H, GPa	E, GPa	R, %
Copper	2.1	121	14
Titan	4.1	130	19
The multilayer film Ti/α-C:H	8.0	128	34
The amorphous ribbon Zr–Cu–Ti–Ni	11.5	117	42
Silicon (100)	11.8	174	62
Thin film Ti–Si–N	28.4	295	62

Vickers microhardness coating Cr–Mn–Si–Cu–Fe–Al argon is 133.8 HV, and coating Cr–Mn–Si–Cu–Fe–Al–Ti in a nitrogen environment — 328.0 HV, ie it increased by almost 2.5 times. The sharp increase in

the microhardness cover Cr–Mn–Si–Cu–Fe–Al–Ti, deposited in a nitrogen atmosphere, associated with the formation of nitride phases. In general, these titanium nitride and chromium.

Influence of technological parameters on the fracture energy of coatings

The direct impact on the structure and physical properties of the coatings obtained by ion-plasma deposition, provide the following parameters: the pressure of the reaction gas in the chamber; the potential of the substrate; discharge current of the arc; material properties of the cathode; substrate temperature. The surface tension of a solid σ is the specific surface energy $E = \sigma \cdot S$ (S — surface area).

The coating will be destroyed if the fracture energy $Ep \approx En$. Thus, breaking energy coating can be evaluated by determining the surface tension. In this paper, the surface tension was determined by the method of [17].

Consider the effect of substrate temperature on fracture energy of composite coatings. The measurement results are shown in Table. 7.

Table 7

The relationship between fracture energy coating on the substrate temperature area of 1 cm^2

Coating	Temperature backing, ºC			Energy failure coatings, J		
Zn–Cu–Al	350	400	450	2.06	2.43	2.14
Cr–Mn–Si–Cu–Fe–Al	350	400	450	6.06	7.11	6.21
Mn–Fe–Cu–Al	350	400	450	3.24	3.67	3.09

The optimum temperature of the substrate for all composite coatings was equal to about 400 ºC. Milling grain structure of the coating material with increased substrate temperature accompanied by an increase in hardness and surface tension to a critical average grain size. Reduced hardness with further decrease of average grain size in the coating is due to the slippage at the grain boundaries (rotating effect). Consider the effect of the current arc on the properties of composite coatings. The results are shown in Table 8.

Table 8

The relationship between fracture energy coating on the arc current

Coating	Arc current evaporator, A				Energy failure coatings, J			
Zn–Cu–Al	30	50	70	90	2.43	2.31	2.29	2.27
Cr–Mn–Si–Cu–Fe–Al	30	50	70	90	7.11	6.97	6.95	6.92
Mn–Fe–Cu–Al	30	50	70	90	3.67	3.42	3.12	3.08

Increasing the arc current discharge increases the coating thickness, but with increasing current than 130 A decreases perfection of the structure, and dramatically increases the amount of the droplet phase, which is the cause of reducing the adhesive strength of the coated substrate. At low power discharge (arc current <20–30 A) due to a decrease in the ratio of plasma ionization film «walled up» neutral particles of the reaction gas and the cathode, thereby increasing the concentration of coating defects.

The results of the influence of residual pressure in the vacuum chamber on the properties of the composite coatings are shown in Table 9.

Table 9

Dependence fracture energy coating on the gas pressure chamber

Residual gas pressure in the chamber mm. Hg. Art.	Energy failure coatings, J		
	Zn–Cu-Al	Cr–Mn–Si–Cu–Fe–Al	Mn–Fe–Cu–Al
10^{-8}	2.02	6.32	3.28
10^{-7}	2.11	6.54	3.43
10^{-6}	2.43	7.11	3.67
10^{-5}	2.38	6.87	3.42

After analyzing the results of the study it can be concluded that samples obtained at a nitrogen pressure of $P = 0.081–0.81$ Pa are most evenly distributed small dense structure, the minimum content of the droplet phase, pores, sagging, delamination, and the greatest value of the surface tension.

From the above investigation results, it follows that the production of coatings with desired properties is possible under the main process parameters of the deposition process. Qualitative evaluation of coating properties can be obtained by knowing their surface energy, the melting temperature and the concentration of the respective components or phases in the coating.

Closing

In the case of small lots of parts, and to critical parts of machines and mechanisms is better to use titanium nitride coating, which in addition to enhancing the corrosion resistance, have high strength. The vacuum nitriding a cheaper way to increase corrosion resistance, however, it has certain advantages and to zinc and chrome-plated front.

References

1 *Huang J.H., Yang H.C., Guo X.J., Yu G.P.* Effect of film thickness on the structure and properties of nanocrystalline ZrN thin films produced by ion plating // Surface and Coatings Technology. — 2005. — Vol. 195. — P. 204–213.

2 *Meng Q.N., Wen M., Qu C.Q. et al.* Preferred orientation, phase transition and hardness for sputtered zirconium nitride films grown at different substrate biases // Surface and Coatings Technology. — 2011. — Vol. 205. — P. 2865–2870.

3 *Rea M.D., Gouttebaron R., Dauchot J.-P. et al.* Study of ZrN layers deposited by reactive magnetron sputtering // Surface and Coatings Technology. — 2003. — Vol. 174–175. — P. 240–245.

4 *Zeman P., Cerstvry R., Mayrhofer P.H. et al.* Structure and properties of hard and superhard Zr–Cu–N nanocomposite coatings // Materials Science and Engineering. — 2000. — A289. — P. 189–197.

5 *Sheng S.H., Zhang R.F., Veprek S.* Phase stabilities and thermal decomposition in the $Zr_{1-x}Al_xN$ system studied by ab initio calculation and thermodynamic modeling // Acta Materialia. — 2008. — Vol. 56. — P. 968–976.

6 *Musila J., Karvankova P., Kasl J.* Hard and superhard Zr–Ni–N nanocomposite films // Surface and Coatings Technology. — 2001. — Vol. 139. — P. 101–109.

7 *Suna J., Musil J., Ondok V., Han J.G.* Enhanced hardness in sputtered Zr–Ni–N films // Surface and Coatings Technology. — 2006. — Vol. 200. — P. 6293–6297.

8 *Musil J., Danie R.* Structure and mechanical properties of magnetron sputtered Zr–Ti–Cu–N films // Surface and Coatings Technology. — 2003. — Vol. 166. — P. 243–253.

9 *Musil J., Polakova H.* Hard nanocomposite Zr–Y–N coatings, correlation between hardness and structure // Surface and Coatings Technology. — 2000. — Vol. 127. — P. 99–106.

10 *Daniel R., Musil J., Zeman P., Mitterer C.* Thermal stability of magnetron sputtered Zr–Si–N films // Surface and Coatings Technology. — 2006. — Vol. 201. — P. 3368–3376.

11 *Xueliang Q., Yanhong H., Yiping W., Jianguo Ch.* Study on functionally gradient coatings of Ti–Al–N // Surface and Coatings Technology. — 2000. — Vol. 131. — P. 462–464.

12 *Scheerer H., Hoche H., Broszeit E. et al.* Effects of the chromium to aluminum content on the tribology in dry machining using (Cr, Al)N coated tools // Surface and Coatings Technology. — 2005. — Vol. 200. — P. 203–207.

13 *Brizuela M., Garcia-Luisa A., Braceras I. et al.* Magnetron sputtering of Cr(Al)N coatings: Mechanical and tribological study // Surface and Coatings Technology. — 2005. — Vol. 200. — P. 192–197.

14 *Monclus M.A., Baker M.A., Tsotsos C. et al.* Investigation of the nanostructure and post-coat thermal treatment of wear-resistant PVD (Cr–Ti–Cu–B)N coatings // Surface and Coatings Technology. — 2005. — Vol. 200. — P. 310–314.

15 *Wang L., Niea X., Housden J. et al.* Material transfer phenomena and failure mechanisms of a nanostructured Cr-Al-N coating in laboratory wear tests and an industrial punch tool application // Surface and Coatings Technology. — 2008. — Vo. 203. — P. 816–821.

16 *Li X., Li C., Zhang Y. et al.* Tribological properties of the Ti–Al–N thin films with different components fabricated by double-targeted co-sputtering // Applied Surface Science. — 2010. — Vol. 256. — P. 4272–4279.

17 *Guchenko S.A., Jurov V.M., Laurynas V.Ch., Zavatskiy O.N.* Surface tension of deposited coatings // International Congress on Energy Fluxes and Radiation Effects. — Tomsk: Pub. House of IAO SB RAS, 2014. — P. 389.

Е.С.Платонова, В.Бучинскас, В.М.Юров, В.Ч.Лауринас

Тау-кен құрал-жабдықтар бөлшектерін өндіруде коррозияға төзімді тұндыру технологиясы мен сызаттарға төзімді жабындылар

Мақалада тәжірибеде көрсетілгендей, вакуумдық азоттану технологиясы әлдеқайда мырыш жабындысынан жоғары. Сонымен қатар осындай жабындысы бар бөлшектер құны 10–15 % мырыштан төмен. Төменгі сұрыпты болат бойынша коррозияға төзімді, үйкеліске қарсы жабынды ретінде бұл эксперименттік деректер Fe–Al және Fe–Al–Ti жабындылары пайдаланылуы мүмкін. Бұл 3–4 есе осы болаттардың компоненттердің мерзімін ұзартады. Белгілі қатты материалдармен (7,413 ГПа)

наноқаттылық бойынша алынған нәтижесін салыстыруда, Cr–Mn–Si–C–Fe–Al наноқаттылық жабындысы титанның наноқаттылығынан 2 есе жоғары және Ti/α-C:H көпқабатты қабықтарға жақын. Fe–Al микроқаттылығымен жабындылардың өлшеу нәтижелерін салыстыру Fe–Al–Ti және басқа да көп қабатты жабындысы айтарлықтай жоғары екенін көрсетеді.

Е.С.Платонова, В.Бучинскас, В.М.Юров, В.Ч.Лауринас

Технология осаждения коррозионно-стойких и упрочняющих покрытий на детали горношахтного оборудования

В работе экспериментально показано, что технология вакуумного азотирования значительно превосходит цинковые покрытия. Наряду с этим, себестоимость деталей с такими покрытиями на 10–15 % ниже цинковых. Из экспериментальных данных следует, что покрытия Fe–Al и Fe–Al–Ti могут быть использованы как коррозионно-стойкие, жаропрочные, антифрикционные покрытия на низкосортные сорта стали. При этом увеличивается срок службы деталей из этих сталей в 3–4 раза. Сравнение полученного результата по нанотвердости (7,413 ГПа) с известными твердыми материалами показывает, что нанотвердость покрытия Cr–Mn–Si–Cu–Fe–Al почти в 2 раза выше нанотвердости титана и близка к нанотвердости многослойной пленки Ti/α-C:H. Сравнение результатов измерений с микротвердостью покрытий Fe-Al, Fe-Al-Ti и других показывает, что многослойные покрытия значительно превосходят последние. После азотирования микротвердость многослойного покрытия увеличивается.